

# The soft x-ray instrument for materials studies at the linac coherent light source x-ray free-electron laser

Cite as: Rev. Sci. Instrum. **83**, 043107 (2012); <https://doi.org/10.1063/1.3698294>

Submitted: 03 February 2012 • Accepted: 07 March 2012 • Published Online: 12 April 2012

W. F. Schlotter, J. J. Turner, M. Rowen, et al.



View Online



Export Citation

## ARTICLES YOU MAY BE INTERESTED IN

[Linac Coherent Light Source soft x-ray materials science instrument optical design and monochromator commissioning](#)

Review of Scientific Instruments **82**, 093104 (2011); <https://doi.org/10.1063/1.3633947>

[Modular soft x-ray spectrometer for applications in energy sciences and quantum materials](#)

Review of Scientific Instruments **88**, 013110 (2017); <https://doi.org/10.1063/1.4974356>

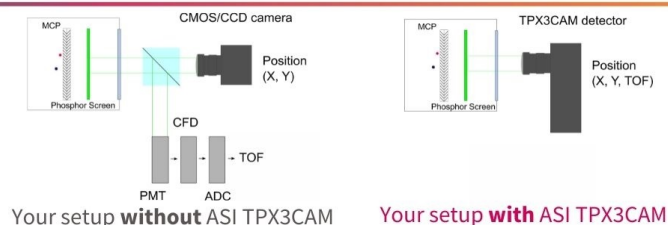
[Development of a compact fast CCD camera and resonant soft x-ray scattering endstation for time-resolved pump-probe experiments](#)

Review of Scientific Instruments **82**, 073303 (2011); <https://doi.org/10.1063/1.3609862>

[www.amscins.com](http://www.amscins.com)



**Simplify Your  
Set-up, Get  
Better Results!**



# The soft x-ray instrument for materials studies at the linac coherent light source x-ray free-electron laser

W. F. Schlotter,<sup>1,a)</sup> J. J. Turner,<sup>1</sup> M. Rowen,<sup>1</sup> P. Heimann,<sup>1,2</sup> M. Holmes,<sup>1</sup> O. Krupin,<sup>1,3</sup> M. Messerschmidt,<sup>1</sup> S. Moeller,<sup>1</sup> J. Krzywinski,<sup>1</sup> R. Soufli,<sup>4</sup> M. Fernández-Perea,<sup>4</sup> N. Kelez,<sup>2,b)</sup> S. Lee,<sup>1,c)</sup> R. Coffee,<sup>1</sup> G. Hays,<sup>1</sup> M. Beye,<sup>5,d)</sup> N. Gerken,<sup>5</sup> F. Sorgenfrei,<sup>5</sup> S. Hau-Riege,<sup>4</sup> L. Juha,<sup>6</sup> J. Chalupsky,<sup>6</sup> V. Hajkova,<sup>6</sup> A. P. Mancuso,<sup>7,e)</sup> A. Singer,<sup>7</sup> O. Yefanov,<sup>7</sup> I. A. Vartanyants,<sup>7,8</sup> G. Cadenazzi,<sup>9</sup> B. Abbey,<sup>9</sup> K. A. Nugent,<sup>9</sup> H. Sinn,<sup>3</sup> J. Lüning,<sup>10</sup> S. Schaffert,<sup>11</sup> S. Eisebitt,<sup>11,12</sup> W.-S. Lee,<sup>13</sup> A. Scherz,<sup>13</sup> A. R. Nilsson,<sup>13</sup> and W. Wurth<sup>5</sup>

<sup>1</sup>LCLS, SLAC National Accelerator Laboratory, 2575 Sand Hill Rd., Menlo Park, California 94025, USA

<sup>2</sup>Advanced Light Source, Lawrence Berkeley National Laboratory, Berkeley, California 94720, USA

<sup>3</sup>European XFEL GmbH, Albert-Einstein-Ring 19, 22761 Hamburg, Germany

<sup>4</sup>Lawrence Livermore National Laboratory, 7000 East Avenue, Livermore, California 94550, USA

<sup>5</sup>Institute for Experimental Physics and CFEL, University of Hamburg, Luruper Chaussee 149, 22761 Hamburg, Germany

<sup>6</sup>Institute of Physics ASCR, Na Slovance 2, 182 21 Prague 8, Czech Republic

<sup>7</sup>Deutsches Elektronen-Synchrotron DESY, Notkestrasse 85, D-22607 Hamburg, Germany

<sup>8</sup>National Research Nuclear University, "MEPhI," 115409 Moscow, Russia

<sup>9</sup>ARC Centre of Excellence for Coherent X-ray Science, School of Physics, The University of Melbourne, Victoria 3010, Australia

<sup>10</sup>Laboratoire de Chimie Physique - Matière et Rayonnement, UMR 7614 CNRS, Université Pierre et Marie Curie, Paris, France

<sup>11</sup>Institut für Optik und Atomare Physik, TU Berlin, Strasse des 17. Juni 135, 10623 Berlin, Germany

<sup>12</sup>Helmholtz-Zentrum Berlin für Materialien und Energie GmbH, Albert-Einstein-Str. 15, 12489 Berlin, Germany

<sup>13</sup>SIMES, SLAC National Accelerator Laboratory, 2575 Sand Hill Rd., Menlo Park, California 94025, USA

(Received 3 February 2012; accepted 7 March 2012; published online 12 April 2012)

The soft x-ray materials science instrument is the second operational beamline at the linac coherent light source x-ray free electron laser. The instrument operates with a photon energy range of 480–2000 eV and features a grating monochromator as well as bendable refocusing mirrors. A broad range of experimental stations may be installed to study diverse scientific topics such as: ultrafast chemistry, surface science, highly correlated electron systems, matter under extreme conditions, and laboratory astrophysics. Preliminary commissioning results are presented including the first soft x-ray single-shot energy spectrum from a free electron laser. © 2012 American Institute of Physics. [<http://dx.doi.org/10.1063/1.3698294>]

## I. INTRODUCTION

Soft x-rays are valued for element and chemical state specific sensitivity as well as probes of nanoscale structure. The electronic structure in chemical reactions or highly correlated electron systems evolves on a sub-picosecond time scale. Therefore, ultrafast pulses of soft x-rays are suited for investigating electrons in materials on their native time scale. The soft x-ray materials research (SXR) instrument was designed to study ultrafast chemistry, clusters as new materials, strongly correlated materials and to perform high-resolution ultrafast coherent imaging on magnetic materials.

The SXR instrument design reflects the need to service a diverse experimental program. Experiments are performed in end stations which house the sample environment and interface to the x-ray beamline, optical pump laser, controls system, and data acquisition system.

Free electron lasers have recently pushed into sub optical wavelengths with FLASH lasing at 6.8 nm in 2007 and 4.1 nm in 2011.<sup>1</sup> Hard x-ray lasing was first achieved at the linac coherent light source (LCLS) in 2009 and SACLA in Japan in 2011 with the European XFEL anticipated to come online in 2015.<sup>2</sup> These sources all rely on the phenomenon of self-amplified spontaneous emission (SASE) to generate high intensity ultrashort x-ray pulses.<sup>3</sup> The SASE process, which relies on the amplification of spontaneously emitted photons, generates pulses with characteristics that fluctuate on each shot. As a result, experiments rely heavily on instrumentation to control or characterize the properties of each free electron laser (FEL) pulse.

This manuscript introduces the SXR instrument in three parts: (1) a comprehensive discussion of the instrument components (2) controls and data acquisition for diverse

<sup>a)</sup>Electronic mail: wschlott@slac.stanford.edu.

<sup>b)</sup>Present address: LCLS, SLAC National Accelerator Laboratory, 2575 Sand Hill Rd., Menlo Park, California 94025, USA.

<sup>c)</sup>Present address: Korea Research Institute of Standards and Science, 267 Gajeong-ro, Yuseong-gu, Daejeon 305-340, Republic of Korea.

<sup>d)</sup>Present address: Helmholtz-Zentrum Berlin für Materialien und Energie GmbH, Albert-Einstein-Str. 15, 12489 Berlin, Germany.

<sup>e)</sup>Present address: European XFEL GmbH, Albert-Einstein-Ring 19, 22761 Hamburg, Germany.

## SXR Beamline Layout

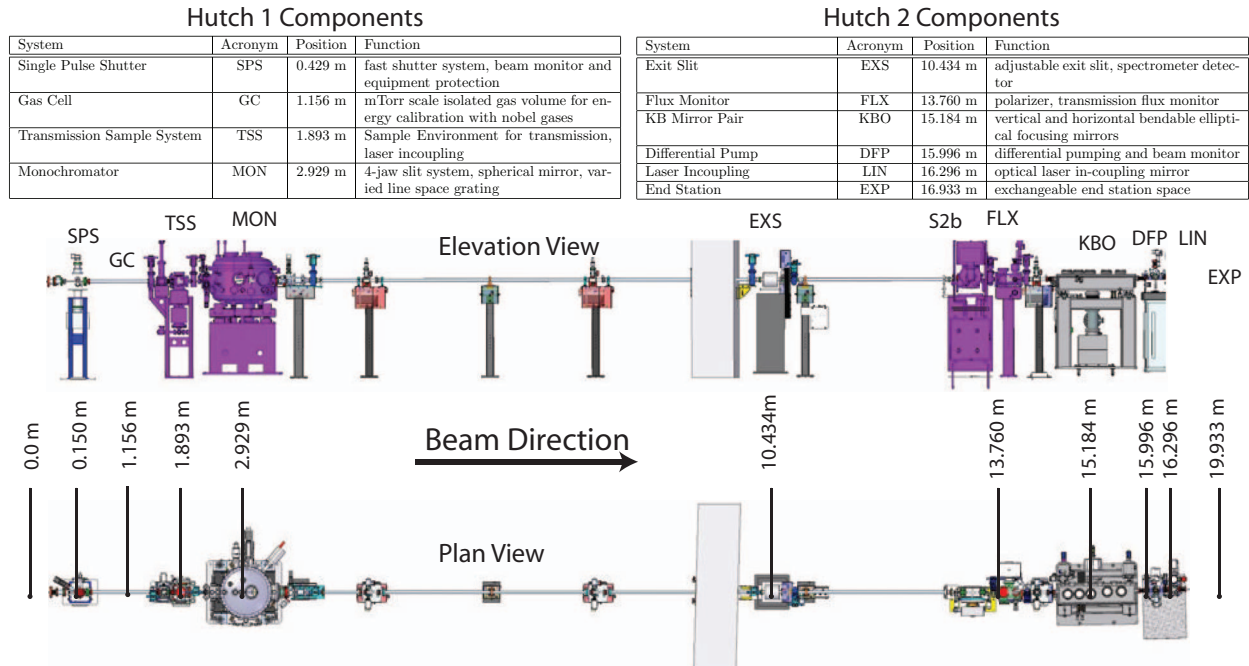


FIG. 1. SXR beamline layout in hutch 1 and hutch 2 of the LCLS Near Experimental Hall. Note that the interface valve denotes the coordinate origin [ $Z = 0.0$  m]. The second photon stopper (S2b) which is located in hutch 2 is introduced in Sec. II A. With S2b closed, access to hutches 1 and 2 is allowed to personnel even with S2 (not shown) open allowing radiation onto S2b. However, because the beam can be focused to a spot exceeding the damage threshold for  $B_4C$  there are no personnel permitted in hutch 2 while S2b is open.

instrumentation and a (3) review of the initial beamline performance measured during commissioning.

## II. LAYOUT AND INSTRUMENT COMPONENTS

The SXR instrument spans two hutches in the Near Experimental Hall of the LCLS at the SLAC National Accelerator Laboratory.<sup>4</sup> Figure 1 illustrates the functional components of the beamline, or instrument, as well as the optical layout. The SXR beamline contains two major optical systems shown together in Figure 1. First, a varied line spacing plane grating monochromator consisting of a focusing mirror, grating system, and exit slit, is located in hutch 1 and the upstream side of hutch 2.<sup>5</sup> The second major optical system is a Kirkpatrick-Baez focusing mirror pair which is located entirely in hutch 2. These major systems are complimented by diagnostics and other systems to form the SXR beamline. This section describes the function and operation of each of the components along the beamline. The first vacuum gate valve of the beamline, or interface valve, in hutch 1 separates the front end enclosure (FEE) systems from the SXR beamline and denotes the coordinate origin [ $Z = 0.0$  m] for the instrumentation. The interface valve is nominally 163.5 m from the x-ray source.<sup>6</sup>

### A. Stoppers and shutters

The first personnel protection photon stopper for the SXR instrument, S2, is housed in the front end enclosure [ $Z = -4.053$  m]. S2, like all LCLS photon stoppers, pneu-

matically inserts two independent stoppers composed of 10.6 mm of  $B_4C$  and 82.5 mm of tungsten. The second SXR photon stopper, S2b, is located in hutch 2. Because the focused LCLS beam can ablate all known solid shielding, permission to open S2 and S2b simultaneously is granted after hutch 2 is searched and cleared of personnel. Without clearing hutch 2 of personnel, S2 can be opened when S2b is closed because containment of the beam is guaranteed by the static shielding and optical geometry. Therefore, personnel can always access hutch 1 during SXR operation.

Directly downstream of the first gate valve of the SXR beamline in hutch 1 is the first component of the SXR beamline, the equipment protection shutter (EPS) [ $Z = 0.150$  m]. In 100 ms the EPS actuates pneumatically by inserting a  $B_4C$  disk that is 3 mm thick and 25 mm in diameter into the beam. The EPS is reliable, robust and can withstand prolonged exposure to the full, unfocused FEL beam without damage.

The single pulse shutter (SPS) [ $Z = 0.429$  m] follows the EPS. The SPS can select individual pulses from the LCLS when the accelerator repetition rate is 10 Hz. As a result any arbitrary sub 10 Hz pulse structure can be delivered without adjusting the accelerator operation. This is important for experiments where a solid fixed target sample needs to be moved into position between FEL pulses as well as experiments where the detector readout time is longer than the period between FEL pulses. The SPS may be operated with a predefined pulse sequence or deliver single pulses on demand. To ensure that the SPS actuation is coincident with the arriving FEL pulse the command to fire is synchronized with a machine event trigger. The SPS is an ultrahigh vacuum

compatible version of the LS055-VBD-NO model laser shutter manufactured by nmLaser of San Jose, CA. The shutter uses a ferromagnetic paddle actuated by an in vacuum water cooled solenoid. For smooth, reliable operation of the SPS a low pass filter ( $\tau = 2.0$  ms) is applied to the drive signal to soften the actuation motion. To avoid prolonged FEL exposure on the closed paddle and to mitigate joule heating in the solenoid, the EPS will close if the SPS is closed for 10 consecutive seconds subsequently allowing the SPS to be retracted from the beam.

A cerium doped YAG crystal can be inserted upstream of the SPS to view the beam profile. This is the first beam diagnostic on the SXR instrument.

## B. Static gas cell

Following the SPS is a static gas cell [ $Z = 1.156$  m] which can be used for energy resolution calibration of the monochromator. The cell is 703 mm long with 200 nm Al filters integrated to the gate of the valves at both the entrance and exit. A 722B11TBA2FK model baratron pressure gauge (MKS Instruments) reports a full scale measurement at a pressure of 10 Torr with an accuracy of 0.5% of the readout value. Limited by the Al filters, the maximum pressure the cell can sustain is 1 Torr. The FEL pulse energy must be limited to approximately  $<40 \mu\text{J}$  for photon energies below 1000 eV to prevent damage to the filters. Chemically inert gases can be injected into the cell which can be fully evacuated to UHV conditions in minutes via a dedicated turbo molecular pump system. After pumping, the gate valves containing the Al filters can be opened rendering the gas cell region transparent.

## C. TSS laser in-coupling and alignment laser

The SXR instrument has two positions where optical laser beams can be incoupled co-linear with the FEL beam. Both use an identically designed system whereby a mirror with an axial hole in the center, to pass the FEL beam, can be inserted at  $45^\circ$  in the horizontal plane with respect to the propagating FEL beam (see Figure 2). The system can accommodate two 50 mm mirrors which typically have a 2 mm axial aperture to transmit the x-ray beam. There is a 14 mm aperture in the mirror mount through which the FEL beam may pass unobstructed. One of the laser in-coupling systems (TSS-LIN) [ $Z = 1.639$  m] is located upstream of the transmission sample system (TSS) described below in Sec. II D, and it can be used to in-couple a pump laser pulse to illuminate a sample in the TSS. An optical breadboard (762 mm  $\times$  610 mm) is located next to the in-coupling to conveniently mount optics for laser beam manipulation. A second LIN system is located at the end of the beamline and will be discussed in Sec. II K.

The TSS LIN is also used to in-couple an alignment laser beam. In this case a  $<0.5$  mW  $\lambda = 543$  nm continuous wave HeNe laser is collimated and directed along the beam path. The alignment laser transmits through the entire beamline and into the end station. Because the alignment laser in-couples the beam 14.526 m upstream of the exit flange and must pass

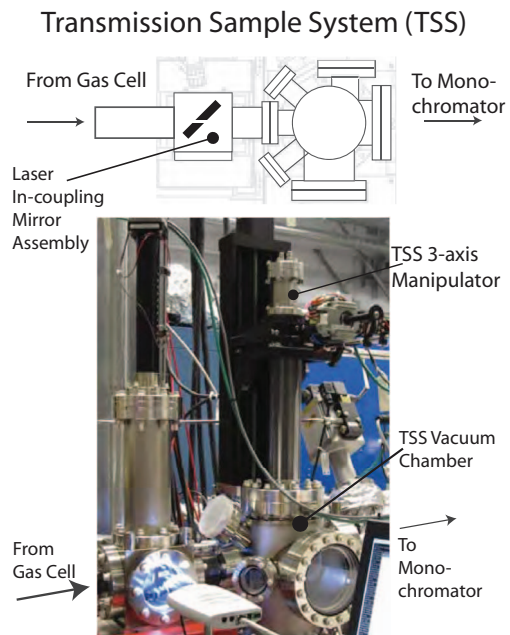


FIG. 2. The transmission sample system (TSS) may be used to introduce transmission samples upstream of the monochromator. It is used for calibrating the wavelength selection of the monochromator but is also available to users for experiments. As shown, the TSS has a single manipulator attached for sample insertion. Additionally, an off center, aft flange allows a detector to be inserted after the sample position at the TSS chamber center (not visible here).

through seven 3.5 mm apertures, the alignment laser path is coincident with the x-ray beam. The alignment laser is useful for optimizing beamline components such as detectors, but its primary application is the ability to see the location of the beam in experimental end stations. Chambers can be aligned and detectors optimized to within 0.5 mm of the x-ray beam position within an end station without using limited FEL beam time.

## D. Transmission sample system

The TSS [ $Z = 1.893$  m] shown in Figure 2 sits downstream of the gas cell, but upstream of the monochromator grating tank. The TSS allows fixed-target transmission samples to be inserted into the FEL beam before any of the beamline optical components. It is one of the experimental stations on the SXR instrument accessible to users via proposal review for experiments. It is also important for the energy calibration of the monochromator whereby x-ray absorption samples of known composition are introduced to the beam in the TSS. At the TSS the beamsizes is 2.1 mm FWHM for a photon energy of 1000 eV which corresponds to an intensity of  $4.5 \times 10^{11}$  W/cm<sup>2</sup> for a FEL pulse energy of 1 mJ and a pulse duration of 50 fs FWHM. The TSS was designed to accommodate a diverse set of experiments. A multi-axis linear translation manipulator is mounted on the TSS to position samples. Off beam axis view ports may be used for cross beam optical laser pulse illumination or to monitor samples. An aft flange allows for detectors to be inserted after the sample position.

## E. Varied line spaced grating monochromator

The SXR instrument is unique between the soft x-ray instruments at the LCLS because of its monochromator.<sup>5,7</sup> Though the energy bandwidth is narrow from the FEL output, less than 0.5% for a typical pulse, the photon energy fluctuates due to the SASE process. The monochromator can both narrow the bandwidth and give the experimenter control over the photon energy. The monochromator mechanical systems were constructed by BesTec GmbH of Berlin, Germany.

The SXR monochromator is designed to work without an additional focus and entrance slit in front of the gratings because the intensity of the FEL beam focused on the entrance slit could easily exceed the B<sub>4</sub>C damage threshold. The beam profile and illumination of the optics can be controlled with four independent slit blades located at the entrance of the monochromator tank [ $Z = 2.289$  m]. Each B<sub>4</sub>C slit blade can be inserted beyond center to fully block the beam or it may be fully removed. To avoid collisions when the blades are inserted completely, each slit blade face is separated by 10 mm in the longitudinal beam direction. Through the controls system, the slits can be moved independently or in tandem pairs.

The grating vacuum vessel houses a spherical mirror (M1) and two varied line space gratings. Both optical substrates are single crystal silicon and the optics were manufactured by Zeiss GmbH. The M1 mirror and the grating, like all of the SXR x-ray optics, consist of a Si substrate coated with a 37.4 nm thick B<sub>4</sub>C reflective coating.<sup>7</sup> The spherical mirror [ $Z = 2.643$  m] has a 1049 m radius of curvature and focuses the beam at the exit slit position. The two varied line space gratings [ $Z = 2.929$  m] have been ruled by Shimadzu in Japan on a single substrate. This allows both a 100 line/mm and 200 line/mm grating to be exchanged simply by a transverse movement of the grating. An area adjacent to the two gratings was left unruled and can be used to directly reflect the beam. The pitch of both the grating and the M1 mirror originate from an out of vacuum linear drive that moves the optical mounting assemblies on a sine bar. Each assembly has two in vacuum angular optical encoders which are averaged to provide feedback control to the drive motors. The feedback is closed loop and only active while the motor is moving to the desired destination. Once the motor arrives at the destination, a holding current is applied such that the position is maintained without the need for feedback from the encoder. This feedback system is implemented for all of the optical components on the beamline.

The output beam can be viewed on a Ce:YAG crystal [ $Z = 3.477$  m]. When the grating is illuminated to allow the first order beam to transmit down the beamline, the unused zero order beam is absorbed by a B<sub>4</sub>C collimator [ $Z = 3.552$  m].

## F. Exit slit and spectrometer detector

The photon energy bandwidth of the dispersed beam is controlled by the exit slit (EXS) [ $Z = 10.434$  m]. The B<sub>4</sub>C exit slit blades are straight to within  $5.6 \mu\text{m}$  over 10 mm and the slit parallelism is 0.36 mrad. This allows the two opposing vertically defining slit blades to close down below  $10 \mu\text{m}$  in a bilateral motion driven by one motor. Because the beam is

vertically focused at the exit slit, the direct (zero order) beam has sufficient intensity to ablate the blades. Therefore, an interlock has been implemented which prevents the beam from being delivered if the exit slit is not open during zero order operation.

The SXR instrument can be operated as a spectrometer when the dispersed beam is directed down the beamline onto a Ce:YAG crystal [ $Z = 10.619$  m] inserted 185 mm after the opened exit slit. The Ce:YAG crystal is illuminated at normal incidence by the FEL. A right angle prism directly after the YAG reflects the signal such that it can be imaged via a camera (Opal 1000, Adimec) and a 70 mm focal length objective. Because the camera can be read out at 120 Hz it is possible to capture a single spectrum for each FEL pulse as shown in Figure 6. This has proven invaluable for characterizing the statistical nature of the FEL radiation. It can also be used for single-shot absorption spectroscopy when a sample is mounted in the transmission sample chamber. Because the LCLS is a short pulse source the monochromator design favors preservation of the short pulse duration over spectral resolution.

The S2b photon stopper follows the EXS as described in Sec. II A. With S2b closed the spectrometer can be conveniently operated without clearing the personnel from hutches 1 or 2.

## G. Polarizer

SASE radiation from the LCLS is horizontally linearly polarized. To generate circularly polarized soft x-rays, magnetic transmission filters [ $Z = 13.900$  m] can be introduced to the beam. Such a filter relies on x-ray magnetic circular dichroism and as a result only functions at specific resonant energies.<sup>8</sup> The polarizer filters are introduced to an *in situ* magnetic field of 0.1 T by a permanent magnet. The angle of the field and the sample can both be adjusted to optimize the degree of circular polarization and the resulting transmission. Typically 4 % of the incident beam is transmitted by the polarizer and the degree of circular polarization is 0.3. When the polarizer is not in use, the filters are removed from the beam.

## H. Fluence monitor

During monochromatic operation, the pulse-to-pulse wavelength fluctuation translates to a fluctuation in flux after the exit slit. As a result the FEE gas detector, which measures the number of photons per pulse before the SXR instrument, is no longer valid for initial intensity normalization.<sup>9</sup> Therefore, an additional solid state fluence monitor [ $Z = 14.017$  m] has been installed downstream of the exit slit.

The monitor measures the shot to shot charge pulse from two 10 nm Al films deposited on both sides of a 200 nm polyimide membrane. The detector transmits a majority of the x-ray flux, the lower limit being 70% transmission at low photon energies (500 eV).

The mount for the fluence monitor membranes is electrically isolated and biased to  $-200$  V to mitigate low energy

electron loss. When a soft x-ray pulse impinges on the film, some of the x-rays are absorbed and eject an electron via photoemission which collectively results in a quantifiable electrical charge pulse proportional to the incident number of x-ray photons.

### I. Kirkpatrick-Baez refocusing mirror system

Remarkable intensities of  $1.25 \times 10^{17}$  W/cm<sup>2</sup> can be achieved when the FEL pulses are focused in the SXR end station position. Focusing is accomplished with a bendable Kirkpatrick Baez (KB) [ $Z = 15.184$  m] focusing mirror pair. The mirrors are composed of a single crystal Si substrate coated with a 37.4 nm thick B<sub>4</sub>C film.<sup>7</sup> Bendable mirrors allow the focal position to be shifted resulting in a change in the size of the beam on the sample. Of the two perpendicular focusing elements comprising the KB system, the horizontal focusing mirror (M2) [ $Z = 14.934$  m] is upstream. M2 is nominally 178.5 m from the x-ray source within the undulator and represents the only horizontal focusing optic in the beamline. The vertically focusing mirror (M3) [ $Z = 15.434$  m] generates a 3.33 times demagnified image of the exit slit at the focus. The smallest vertical and horizontal focal spot is generated in the same plane, which is 2.0 m and 1.5 m from the center of M2 and M3, respectively.<sup>10</sup>

### J. Differential pumping system

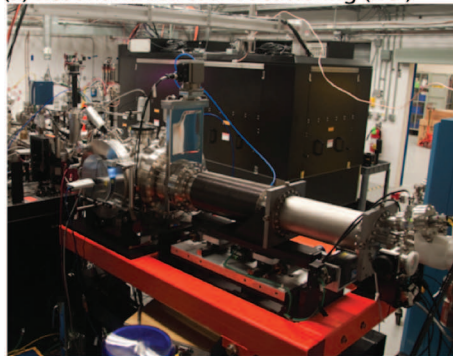
Strict UHV conditions are required where the FEL beam interacts with optical components to avoid cracked hydrocarbons from depositing carbon onto the optics. This is especially true for the KB mirrors which are only 500 mm from the exit flange of the beamline. To relax the vacuum requirements of the end station systems, a differential pumping stage is integrated to the SXR beamline directly after the KB mirrors. A 45 l/s ion pump located between two differential pumping tubes, which are 4.57 mm in diameter and 66.5 mm long, provides nearly two orders of magnitude difference in pressure between the two ends of the system, allowing the pressure in the end station to be as high as  $10^{-6}$  Torr. A residual gas analyzer samples the vacuum near the ion pump in order to monitor the partial pressure of potential hydrocarbons before the gate valve to the optical components of the beamline.

### K. Laser in-coupling system

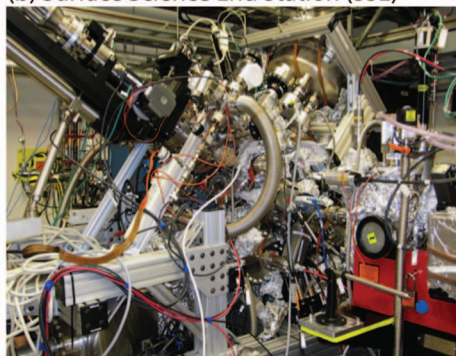
Many ultrafast pump-probe experiments require collinear pump and x-ray beams. A duplicate of the system described in Sec. II C, the LIN [ $Z = 16.296$  m], is the last component upstream of the end station. To allow for a large 50 mm optical beam size, the exit gate valve for the beamline is actually

## SXR End Station Systems

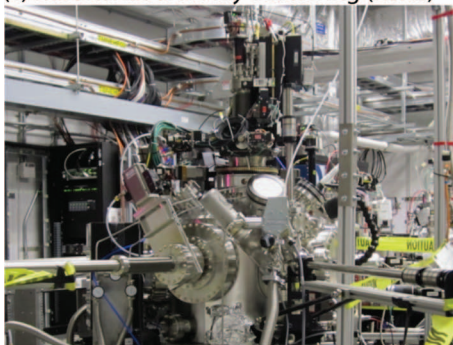
(a) Resonant Coherent Scattering (RCI)



(b) Surface Science End Station (SSE)



(c) Resonant Soft X-ray Scattering (RSXS)



(d) Liquid Jet End Station (LJE)

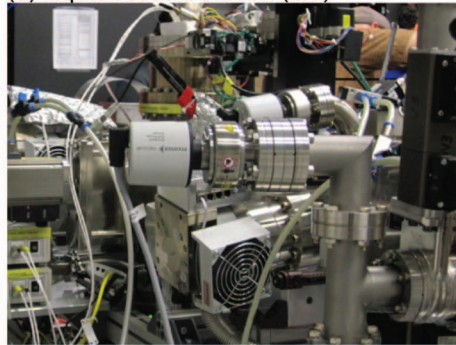


FIG. 3. End stations integrated for operation on the SXR instrument: (a) The resonant coherent imaging (RCI) end station features precision in vacuum sample manipulation and a soft x-ray sensitive CCD camera. It is optimized for coherent scattering experiments. (b) The surface science end station (SSE) features a sample manipulation system as well as an x-ray emission spectrometer and a hemispherical electron analyzer. It is intended for studying the chemical dynamics at surfaces and interfaces. (c) The resonant soft x-ray scattering (RSXS) end station features a cryostat with precision sample manipulation and a CCD camera that can read out one frame for each x-ray pulse.<sup>17</sup> It is designed for soft x-ray diffraction to study correlated systems like high Tc superconductors. (d) The liquid jet end station (LJE) features a liquid jet sample injection system and a grating spectrometer. The LJE is used to study liquid phase chemistry.

upstream of the laser in-coupling system. As a result the user end stations may connect directly to the laser in-coupling system, which has an integrated turbo molecular pump and multiple pressure gauges.

## L. Experimental end stations

The SXR instrument was designed to accommodate a wide range of sample environments, experimental geometries, and detection methods. Such flexibility is enabled by exchanging entire experimental systems or end stations. Unlike other LCLS instruments, there is no dedicated end station on SXR, instead a 10 m<sup>2</sup> area of the hutch downstream of the exit flange is void of any permanent equipment. The nominal exit flange for the beamline is at  $Z = 16.456$  m, while the nominal focus for the KB mirrors is at  $Z = 16.933$  m. The area is designed for rapid and simple exchanges of instrumentation. In addition to the commissioning end station there are four other end stations described in Figure 3.

## M. Commissioning end station

A simple end station shown in Figure 4 was constructed to measure the focal spot size, flux, and demonstrate laser to x-ray pulse timing synchronization. The end station features a 254 mm diameter spherical UHV vacuum chamber. Two three-axis manipulators (McAllister MB1500) were used to position samples and detectors at the center of the chamber. Samples were imaged with 5  $\mu$ m resolution on axis using a 45° incidence angle optical mirror with an axial hole to transmit x-rays viewed by a long working distance microscope. The entire vacuum system could be translated 30 cm along the beam path to measure the depth of focus of the KB mirror system.

## N. Pulse monitoring system

For experiments where the FEL beam is transmitted through the end station, a pulse-by-pulse monitoring system is installed downstream of the end station system. The vacuum vessel for the pulse monitoring system has a dedicated turbo molecular pump, and the entire system has a mechanical support that is independent of the end station. Various diodes are introduced to the beam, but because of the high FEL intensity a set of absorption filters directly upstream of the diodes attenuate the FEL to prevent saturation of the diode signal level. The monitor vessel also has space for a calorimeter. The extreme downstream flange is the terminus for the FEL beam so a B<sub>4</sub>C disk that is 4.8 mm thick and 82.5 mm in diameter is integrated to the flange to serve as a photon beam dump.

## III. CONTROLS AND DATA ACQUISITION (DAQ)

Unlike a synchrotron light source, the peak brightness of the LCLS is sufficient to ablate steel or glass shielding when the soft x-ray beam is highly focused. As a result, personnel are restricted from the experimental hutches when focused radiation is present. Operationally, this requires remote control

## Commissioning End Station

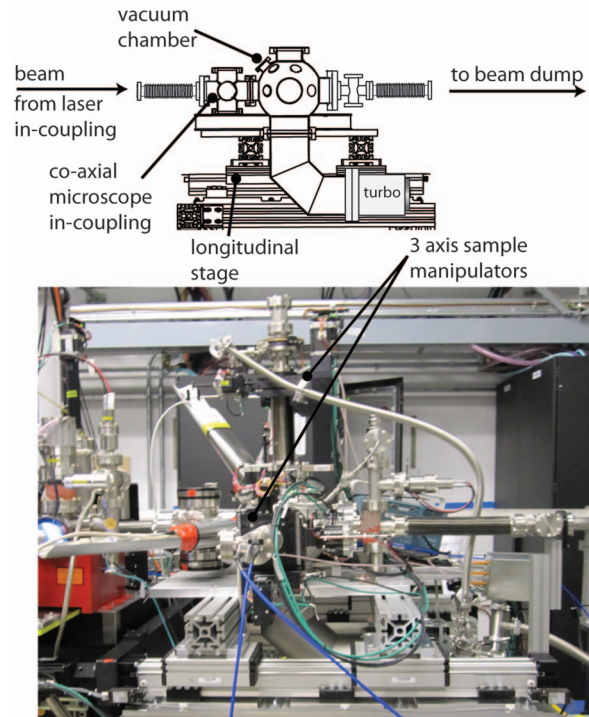


FIG. 4. The commissioning end station is a spherical vacuum vessel on an extruded aluminum frame. A long travel linear rail system moves the entire chamber system in the longitudinal beam direction. Welded bellows up and downstream of the chamber allow the vacuum system to accommodate for the long linear travel of the chamber in the longitudinal beam direction.

of the mechanical motion, vision, vacuum, and data acquisition systems. Moreover, the cost and scarcity of LCLS beam-time encourages the efficiency enabled by full remote control of the instrument.

## A. Controls and DAQ

A comprehensive controls and data acquisition system based on programmable logic controllers (PLCs), experimental physics interface controls system (EPICS) and an event-by-event synchronized data acquisition system developed at SLAC is employed on the SXR instrument. Critical machine protection and vacuum component control such as gate valves must be fast and reliable: therefore, they are monitored and commanded by programmable logic controllers. Non-critical beamline components such as motor motion, camera vision, and pneumatic drive systems do not have strict schedule or speed requirements. Therefore, they are controlled and addressed via software input output controllers operating on Linux computers located in hutch 2. The EPICS typically updates commands ten times per second regardless of the repetition rate of the accelerator.

Detectors which must readout once for each FEL pulse at 120 Hz are part of the data acquisition (DAQ) system which operates on an independent network. The DAQ system stores beamline data (BLD) for each shot. Examples of BLD are the charge of the electron bunch, the photon pulse energy as measured by the FEE gas detectors as well as the arrival time of

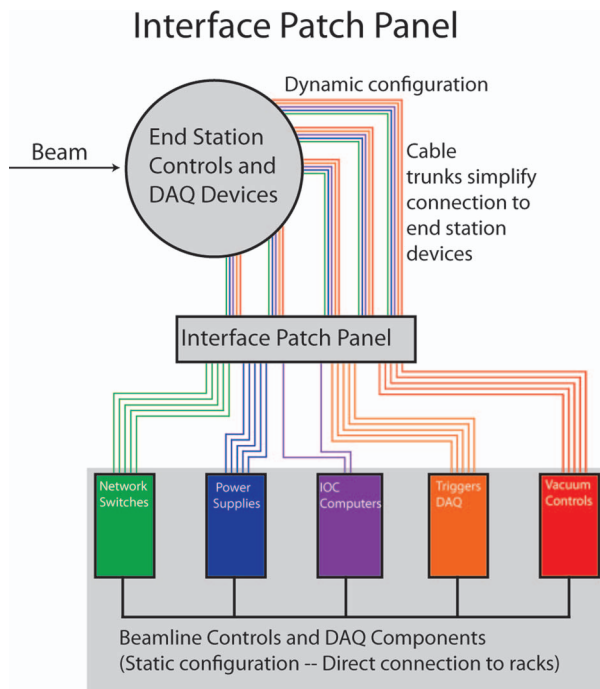


FIG. 5. A block diagram of the controls system and connection interface for end station integration. Each end station uses a dedicated set of cables to connect end station devices to the interface panel. This enables simple access to the controllers and devices distributed over seven racks within hutch 2.

the electron bunch at the end of the undulator. Individual values such as the charge integrated by a single point detector or the position of an optical encoder can be recorded on a shot-to-shot basis by the DAQ. Arrays of data associated with each shot are recorded in the DAQ and may be acquired as a time trace from a voltage digitizer or an image readout from a camera. The entire system is used to control and record data for both the SXR beamline and the end stations connected to it.

### B. Connection interface patch panel

While the controls and DAQ system for the beamline are static, end stations may be changed entirely within 48 h. Controls and DAQ integration for the end stations is simplified by a dedicated connection interface located in hutch 2 in close proximity to the end station space. The interface racks provide simple access to: vacuum gauge controllers, high voltage power supplies, network switches, motion controllers, detector drivers, fast digitizers, and many other devices located in fully enclosed water cooled electronics racks distributed around the experiment hall. The connector interface was designed to make equipment change over simple and efficient (see Figure 5). For example, the power, signal, trigger, and illumination connectors needed to operate a camera are grouped together on the interface panel. An exact duplicate of the controls system including the interface panel is located in a setup laboratory space adjacent to the experimental hutch. This allows users to configure devices and test controls systems before occupying the end station area in the experimental hutch.

## IV. LASER SYSTEM

For pump-probe experiments, an 800 nm titanium doped sapphire oscillator and regenerative amplifier is capable of delivering 3.5 mJ pulses with a 50 fs duration at 360 Hz. The oscillator and amplifier are located above the hutch in a dedicated laser laboratory and the beam is delivered to the optical table in hutch 2 via an evacuated pipe. The pulses are compressed, delayed, and otherwise conditioned on the optical table before delivery to the experimental end stations.

## V. COMMISSIONING RESULTS AND BASELINE PERFORMANCE

Commissioning of the SXR instrument began with first light on May 6, 2010 and lasted until the first user experiment on July 1, 2010. Initial results during this commissioning period are summarized in this section.

### A. Monochromator

The first single-shot spectra from the LCLS was recorded with the SXR spectrometer and is shown in Fig. 6. The structure of the spectrum validates the amplification of noise characteristics of SASE FEL sources. The average of multiple spectra show the mean bandwidth of the FEL is 7 eV

## Single Shot Spectrum

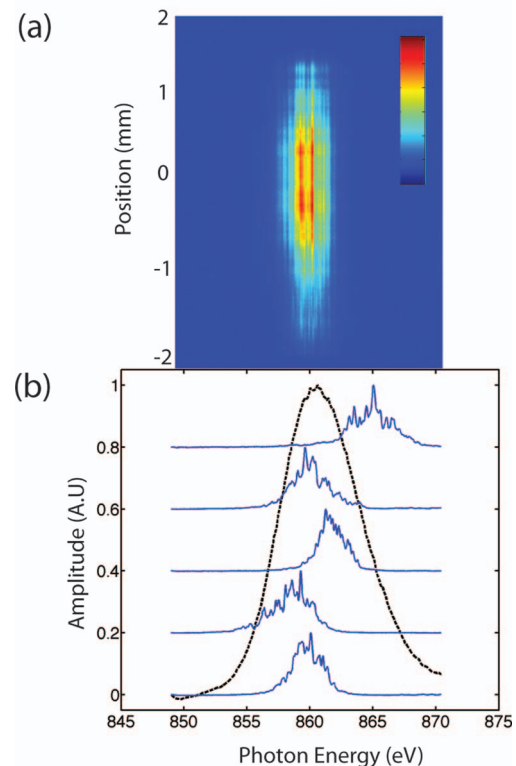


FIG. 6. (a) The first image of a single-shot spectrum produced by a free electron laser at soft x-ray energies. The vertical axis is the horizontal extent of the beam with the energy dispersion in the horizontal axis. The horizontal axis for (b) is shared with (a). (b) Plots of the spectra are generated by projecting the center 2 mm of (a) thus averaging over the extent of the beam. Five characteristic single-shot spectra are normalized, offset and shown in blue and the average of 3000 spectra is shown in black.

(FWHM) with a central energy of 862 eV. This average bandwidth is composed of the intrinsic bandwidth of each pulse as well as the pulse to pulse variation in central energy resulting from jitter in the electron beam energy.

The resolving power of the monochromator was measured using the  $1s-3p$  absorption resonance of Ne at 867 eV.<sup>5</sup> The resolving power,  $\Delta E/E$  of the 100 line/mm and 200 line/mm gratings are 2000 and 3500, respectively. The absolute photon wavelength was calibrated using the monochromator and a set of transmission samples in absorption.

## B. Intensity

The fluence of each FEL pulse presents a novel detection challenge because x-ray detectors can easily saturate from the high intensity. A suite of detection schemes was used to validate linearity and detector performance. A gas detector located in the FEE, upstream of the entire beamline, measures the number of photons in each pulse and transmits the beam.<sup>4,9</sup> The solid state fluence monitor was tested on the SXR instrument downstream of the exit slit of the monochromator and is capable of measuring pulse energies down to the microjoule level. For example, the fluence monitor reported an energy of  $1.9 \pm 0.3 \mu\text{J}$  per pulse with a signal to noise ratio of 7; this measurement was made at 645 eV with a FEL pulse energy of 0.8 mJ with the monochromator in first order using the 100 line/mm grating and an exit slit spacing of  $5 \mu\text{m}$ .

An absolute gas detector developed at DESY was installed downstream of the commissioning end station and upstream of the monitor tank. X-rays incident on the detector ionize gas atoms, here Kr and Xe were used independently, and the ions are extracted by a 2 kV potential. The ion signal is filtered before integration and is proportional to the average number of photons over a 30 s period. The measured transmission of the beamline at 800 eV was  $22\% \pm 2\%$  of the energy originating from the undulator.<sup>11</sup>

## C. Focus

The focal position of the x-ray beam in the end station area can be adjusted with a bendable KB mirror system. To achieve the nominal focal position and thus the smallest focal spot, the mirrors are bent to their minimum radius. The resulting focal position is 0.5 m downstream of the exit flange with an experimentally measured spot size of  $13.2 \mu\text{m}^2$  at 1600 eV with the monochromator operating in zeroth order mode.<sup>12</sup>

The mirrors can be bent independently of the insertion and pitch which is adjusted by the motion of the mirror stand. Aligning the beam to the center of both mirrors was accomplished with the five-degree of freedom motion of the stand.

Achieving the smallest possible spot size requires a coincident longitudinal focus for both KB mirrors. The SXR commissioning chamber was used for optimization and measurement of the focus. Samples, YAG for online focus optimization and  $\text{PbWO}_4$  for focal size imprint measurements, were positioned around the center of the vacuum vessel with three axis manipulators. These samples could be optically examined *in situ* with a point of view co-axial to the

x-ray beam. The entire chamber assembly could be moved along the beam axis and thus through the depth of focus.

Each focal axis was independently improved by bending the optimization mirror and unbending the other to create a line focus. In this way the intensity on the YAG screen remained below the damage threshold. The bend of each mirror and longitudinal position of YAG screen were iteratively varied to reach the optimal focus parameters.

Measurement of the actual focal spot size when both mirrors are bent was done by recording an imprint of the beam in a  $\text{PbWO}_4$  substrate. The array of single-shot imprints in  $\text{PbWO}_4$  was inspected with an *ex situ* differential interference contrast microscope. The depth of focus was found to be 13.4 mm.<sup>12,13</sup>

## D. Timing

Many of the experiments planned for the SXR instrument are optical-pump x-ray-probe. Such experiments require that the pulse can be synchronized and precisely delayed. The synchronization of the optical laser using the machine trigger distribution system is controllable to within 8.4 ns. Picosecond synchronization can be rapidly achieved with a 13 GHz oscilloscope observing the signal generated by each laser pulse on a high bandwidth detector. An SMA type connector serves as the same detector for both x-rays and the high intensity optical pulse (see Figure 7). Fine adjustments to the

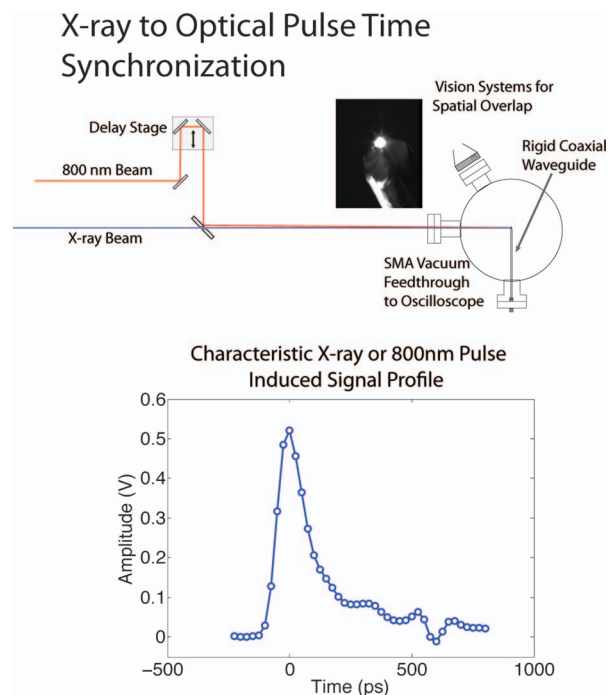


FIG. 7. Temporal overlap between the x-ray and optical pulses must be established for each experiment and monitored. Here, a simple and robust method for achieving sub 5 ps temporal overlap is illustrated. A rigid coaxial rf cable was terminated such that the center conductor comes to point which can be illuminated by both the optical and x-ray beam. The cable terminates in an SMA connector which is attached to a 25 GHz vacuum feedthrough (Times Microwave System P/N 59 130). The sufficient bandwidth is maintained through the transmission to take full advantage of the 13 GHz input bandwidth of the oscilloscope (LeCroy WAVEMASTER 813ZI).

optical delay stage enable sub 5 ps synchronization using this method. For femtosecond synchronization, a simple pump-probe configuration is used where the optical laser arrival delay is scanned. For example, the 800 nm change in reflectivity from a thin (sub-micrometer) silicon nitride film pumped by an x-ray laser pulse is a simple and effective method for establishing precise time overlap.<sup>14,15</sup>

## E. Coherence

Quantifying the unprecedented transverse coherence of the LCLS x-ray pulse is important to accommodate coherent diffraction imaging, x-ray photon correlation spectroscopy and holography experiments. Nano-fabricated double pinhole transmission masks were used to characterize the transverse coherence properties of the beam. The pinholes were 340 nm in diameter separated by 2  $\mu\text{m}$  to 15  $\mu\text{m}$ . These samples were introduced to a 17  $\mu\text{m}$  focal spot and a single x-ray pulse illuminated the nano-structured sample creating the scattering pattern. The fringe visibility of the scattering patterns from the pinholes as a function of pinhole separation was extracted to generate a modulus of the complex degree of coherence. The horizontal transverse coherence length measured at 780 eV was 17  $\mu\text{m}$ .<sup>16</sup> From these measurements the total degree of transverse coherence is 56% and that the x-ray pulses are adequately described by two transverse coherent modes in each direction. This leads to the conclusion that 78% of the total power is present in the dominant mode.<sup>16</sup>

## VI. SUMMARY

In summary, the SXR instrument on the LCLS is operational for users to study materials with ultrafast monochromatic soft x-rays. Preliminary commissioning results from the SXR instrument demonstrate the capability to perform experiments on the frontiers of physics, chemistry, and materials science.

## ACKNOWLEDGMENTS

This research was carried out on the SXR Instrument at the Linac Coherent Light Source (LCLS), a division of SLAC National Accelerator Laboratory and an Office of Science user facility operated by Stanford University for the U.S. Department of Energy (DOE). The SXR Instrument is funded by a consortium whose membership includes the LCLS, Stanford University through the Stanford Institute for Materials Energy Sciences (SIMES), Lawrence Berkeley National Laboratory (LBNL), University of Hamburg through the BMBF priority program FSP 301, and the Center for Free Electron Laser Science (CFEL). In addition this work was performed under the auspices of the U.S. Department of Energy by Lawrence Livermore National Laboratory under Contract No. DE-AC52-07NA27344. V.H., J.C., and L.J. appreciate financial support from the Czech Science Foundation within the grant P108/11/1312. The authors would like to thank Zahid Hussain and Jo Stöhr for guidance on this project.

- <sup>1</sup>W. Ackermann, G. Asova, V. Ayvazyan, A. Azima, N. Baboi, J. Baehr, V. Balandin, B. Beutner, A. Brandt, A. Bolzmann, R. Brinkmann, O. I. Brovko, M. Castellano, P. Castro, L. Catani, E. Chiadroni, S. Choroba, A. Cianchi, J. T. Costello, D. Cubaynes, J. Dardis, W. Decking, H. Delsim-Hashemi, A. Delsierieys, G. Di Pirro, M. Dohlus, S. Duesterer, A. Eckhardt, H. T. Edwards, B. Faatz, J. Feldhaus, K. Floettmann, J. Frisch, L. Froehlich, T. Garvey, U. Gensch, C. Gerth, M. Goerler, N. Golubeva, H.-J. Grabosch, M. Grecki, O. Grimm, K. Hacker, U. Hahn, J. H. Han, K. Honkavaara, T. Hott, M. Huening, Y. Ivanisenko, E. Jaeschke, W. Jalmuzna, T. Jezynski, R. Kammering, V. Katalov, K. Kavanagh, E. T. Kennedy, S. Khodyachykh, K. Klose, V. Kocharyan, M. Koerfer, M. Kollwe, W. Koprek, S. Korepanov, D. Kostin, M. Krassilnikov, G. Kube, M. Kuhlmann, C. L.S. Lewis, L. Lilje, T. Limberg, D. Lipka, F. Loehl, H. Luna, M. Luong, M. Martins, M. Meyer, P. Michelato, V. Miltchev, W. D. Moeller, L. Monaco, W. F.O. Mueller, O. Napieralski, O. Napoly, P. Nicolosi, D. Noelle, T. Nunez, A. Oppelt, C. Pagani, R. Paparella, N. Pchalek, J. Pedregosa-Gutierrez, B. Petersen, B. Petrosyan, G. Petrosyan, L. Petrosyan, J. Pflueger, E. Ploenjes, L. Poletto, K. Pozniak, E. Prat, D. Proch, P. Pucyk, P. Radcliffe, H. Redlin, K. Rehlich, M. Richter, M. Roehrs, J. Roenssch, R. Romaniuk, M. Ross, J. Rossbach, V. Rybnikov, M. Sachwitz, E. L. Saldin, W. Sandner, H. Schlarb, B. Schmidt, M. Schmitz, P. Schmueser, J. R. Schneider, E. A. Schneidmiller, S. Schnepp, S. Schreiber, M. Seidel, D. Sertore, A. V. Shabunov, C. Simon, S. Simrock, E. Sombrowski, A. A. Sorokin, P. Spanknebel, R. Spesyvtsev, L. Staykov, B. Steffen, F. Stephan, F. Stulle, H. Thom, K. Tiedtke, M. Tischer, S. Toleikis, R. Treusch, D. Trines, I. Tsakov, E. Vogel, T. Weiland, H. Weise, M. Wellhoeffler, M. Wendt, I. Will, A. Winter, K. Wittenburg, W. Wurth, P. Yeates, M. V. Yurkov, I. Zagorodnov, and K. Zapfe, *Nature Photon.* **1**, 336 (2007).
- <sup>2</sup>P. Emma, R. Akre, J. Arthur, R. Bionta, C. Bostedt, J. Bozek, A. Brachmann, P. Bucksbaum, R. Coffee, F. J. Decker, Y. Ding, D. Dowell, S. Edstrom, A. Fisher, J. Frisch, S. Gilevich, J. Hastings, G. Hays, P. Hering, Z. Huang, R. Iverson, H. Loos, M. Messerschmidt, A. Miahnahri, S. Moeller, H. D. Nuhn, G. Pile, D. Ratner, J. Rzepiela, D. Schultz, T. Smith, P. Stefan, H. Tompkins, J. Turner, J. Welch, W. White, J. Wu, G. Yocky, and J. Galayda, *Nature Photon.* **4**, 641 (2010).
- <sup>3</sup>E. Saldin, E. Schneidmiller, and M. Yurkov, *The Physics of Free Electron Lasers* (Springer, 2000).
- <sup>4</sup>S. Moeller, J. Arthur, A. Brachmann, R. Coffee, F. J. Decker, Y. Ding, D. Dowell, S. Edstrom, P. Emma, Y. Feng, A. Fisher, J. Frisch, J. Galayda, S. Gilevich, J. Hastings, G. Hays, P. Hering, Z. Huang, R. Iverson, J. Krzywinski, S. Lewis, H. Loos, M. Messerschmidt, A. Miahnahri, H. D. Nuhn, D. Ratner, J. Rzepiela, D. Schultz, T. Smith, P. Stefan, H. Tompkins, J. Turner, J. Welch, B. White, J. Wu, G. Yocky, R. Bionta, E. Ables, B. Abraham, C. Gardener, K. Fong, S. Friedrich, S. Hau-Riege, K. Kishiyama, T. McCarville, D. McMahon, M. McKernan, L. Ott, M. Pivovarov, J. Robinson, D. Ryutov, S. Shen, R. Soufli, and G. Pile, *Nucl. Instrum. Methods Phys. Res. A* **635**, S6 (2011).
- <sup>5</sup>P. Heimann, O. Krupin, W. F. Schlotter, J. Turner, J. Krzywinski, F. Sorgenfrei, M. Messerschmidt, D. Bernstein, J. Chalupsky, V. Hajkova, S. Hau-Riege, M. Holmes, L. Juha, N. Kelez, J. Luning, D. Nordlund, M. F. Perea, A. Scherz, R. Soufli, W. Wurth, and M. Rowen, *Rev. Sci. Instrum.* **82**, 093104 (2011).
- <sup>6</sup>This distance to the source is consistent with the commissioning measurements. It is 40 m more than the design distance because of the ten undulators that were converted to second harmonic afterburners and thus were no longer suitable for soft x-rays. It is also important to note that the x-ray source point is dependent on photon energy and the specific undulator configuration.
- <sup>7</sup>R. Soufli, M. Fernández-Perea, S. L. Baker, J. C. Robinson, E. M. Gullikson, P. Heimann, V. V. Yashchuk, W. R. McKinney, W. F. Schlotter, and M. Rowen, "Development and calibration of mirrors and gratings for the Soft X-Ray Materials Science beamline at the LCLS free-electron laser," to be published in *Applied Optics* (2012).
- <sup>8</sup>B. Pfau, C. M. Guenther, R. Koennecke, E. Guehrs, O. Hellwig, W. F. Schlotter, and S. Eisebitt, *Opt. Express* **18**, 13608 (2010).
- <sup>9</sup>S. P. Hau-Riege, R. M. Bionta, D. D. Ryutov, and J. Krzywinski, *J. Appl. Phys.* **103**, 053306 (2008).
- <sup>10</sup>M. Howells and D. Lunt, *Opt. Eng.* **32**, 1981 (1993).
- <sup>11</sup>A. A. Sorokin, U. Jastrow, P. Juranic, S. Kapitzi, K. Tiedtke, M. Richter, U. Arp, J. Turner, W. F. Schlotter, S. Moeller, "Pulse energy monitoring at the SXR beamline using gas-monitor detectors" (unpublished).
- <sup>12</sup>J. Chalupsky, P. Bohacek, V. Hajkova, S. P. Hau-Riege, P. A. Heimann, L. Juha, J. Krzywinski, M. Messerschmidt, S. P. Moeller, B. Nagler,

- M. Rowen, W. F. Schlotter, M. L. Swiggers, and J. J. Turner, *Nucl. Instrum. Methods Phys. Res. A* **631**, 130 (2011).
- <sup>13</sup>V. Hajkova, L. Juha, P. Bohacek, T. Burian, J. Chalupsky, L. Vysin, J. Gaudin, P. Heimann, S. Hau-Riege, M. Jurek, D. Klinger, J. Pelka, R. Sobierajski, J. Krzywinski, M. Messerschmidt, S. Moeller, B. Nagler, M. Rowen, W. Schlotter, M. Swiggers, J. Turner, S. Vinko, T. Whitcher, J. Wark, M. Matuchova, S. Bajt, H. Chapman, T. Dzelzainis, D. Riley, J. Andreasson, J. Hajdu, B. Iwan, N. Timneanu, K. Saksl, R. Faustlin, A. Singer, K. Tiedtke, S. Toleikis, I. Vartanyants, and H. Wabnitz, *Proc. SPIE* **8077**, 807718 (2011), Damage to VUV, EUV, and x-ray optics III, 18-20 April 2011, Prague, Czech Republic.
- <sup>14</sup>C. Gahl, A. Azima, M. Beye, M. Deppe, K. Doeblich, U. Hasslinger, F. Hennies, A. Melnikov, M. Nagasono, A. Pietzsch, M. Wolf, W. Wurth, and A. Föhlisch, *Nature Photon.* **2**, 165 (2008).
- <sup>15</sup>O. Krupin, M. Trigo, M. Beye, F. Sorgenfrei, W. F. Schlotter, J. J. Turner, D. A. Reis, N. Gerken, S. Lee, W. S. Lee, G. Hays, Y. Acremann, B. Abbey, R. Coffee, M. Messerschmidt, S. P. Hau-Riege, G. Lapertot, J. Luning, P. Heimann, S. Regina, M. Fernández-Perea, M. Rowen, M. Holmes, S. Molodtsov, A. Föhlisch, and W. Wurth, "Temporal Cross-Correlation of X-ray Free Electron and Optical Lasers using Soft X-ray Pulse Induced Transient Reflectivity" (unpublished).
- <sup>16</sup>I. A. Vartanyants, A. Singer, A. P. Mancuso, O. M. Yefanov, A. Sakdinawat, Y. Liu, E. Bang, G. J. Williams, G. Cadenazzi, B. Abbey, H. Sinn, D. Attwood, K. A. Nugent, E. Weckert, T. Wang, D. Zhu, B. Wu, C. Graves, A. Scherz, J. J. Turner, W. F. Schlotter, M. Messerschmidt, J. Luning, Y. Acremann, P. Heimann, D. C. Mancini, V. Joshi, J. Krzywinski, R. Soufli, M. Fernández-Perea, S. Hau-Riege, A. G. Peele, Y. Feng, O. Krupin, S. Moeller, and W. Wurth, *Phys. Rev. Lett.* **107**, 144801 (2011).
- <sup>17</sup>D. Doering, Y. D. Chuang, N. Andresen, K. Chow, D. Contarato, C. Cummings, E. Domning, J. Joseph, J. S. Pepper, B. Smith, G. Zizka, C. Ford, W. S. Lee, M. Weaver, L. Pattthey, J. Weizeorick, Z. Hussain, and P. Denes, *Rev. Sci. Instrum.* **82**, 073303 (2011).